

# A NEW LED-LED PORTABLE CO<sub>2</sub> GAS SENSOR BASED ON AN INTERCHANGEABLE MEMBRANE SYSTEM FOR INDUSTRIAL APPLICATIONS

## Abstract

A new system for CO<sub>2</sub> measurement (0-100%) by based on a paired emitter-detector diode arrangement as a colorimetric detection system is described. Two different configurations were tested: *configuration 1* (an opposite side configuration) where a secondary inner-filter effect accounts for CO<sub>2</sub> sensitivity. This configuration involves the absorption of the phosphorescence emitted from a CO<sub>2</sub>-insensitive luminophore by an acid-base indicator and *configuration 2* wherein the membrane containing the luminophore is removed, simplifying the sensing membrane that now only contains the acid-base indicator. In addition, two different instrumental configurations have been studied, using a paired emitter-detector diode system, consisting of two LEDs wherein one is used as the light source (emitter) and the other is used in reverse bias mode as the light detector. The first configuration uses a green LED as emitter and a red LED as detector, whereas in the second case two identical red LEDs are used as emitter and detector. The system was characterised in terms of sensitivity, dynamic response, reproducibility, stability and temperature influence. We found that configuration 2 presented a better CO<sub>2</sub> response in terms of sensitivity.

**Key words.** Carbon dioxide sensor; Gas sensor; Optical sensor; Paired emitter detector-diode sensor; Portable instrumentation.

## 1. INTRODUCTION

CO<sub>2</sub> is an important industrial gas for many different uses that include production of chemicals (e.g. urea), inert agent for food packaging (to extend the shelf-life of meat, cheese, etc.), beverages, refrigeration systems, welding systems, fire extinguishers, water treatment processes, and many other smaller scale applications [1;2].

In the agro-food industry CO<sub>2</sub> is widely used in modified-atmosphere packaging where its task is to inhibit growth of spoilage bacteria [3;4]. For instance, in active packaging technologies a CO<sub>2</sub> generating system can be considered as a technique complimentary to oxygen scavenging [5]. High CO<sub>2</sub> levels (10-80 %) are desirable for foods such as meat and poultry in order to inhibit surface microbial growth and to extend their life time. The maintenance of CO<sub>2</sub> concentration within packages in food [6], as instance using inserted sachets [7;8], must be carefully monitored since CO<sub>2</sub> permeability is 3-5 times higher than that of oxygen for most of the plastic films and because CO<sub>2</sub> is absorbed by many foods like meat and poultry.

Real-time process monitoring is fundamental for effective process control. The rapid development of bioprocess applications together with the agro-food industry have led to an intensive search for new sensors capable of providing real-time information about the state of the processes.

Conventional methods for CO<sub>2</sub> determination include, among others, infrared spectrometry [9] or electrochemical sensors based on liquid (Severinghaus-type electrodes) or solid electrolytes [10;11]. The most popular sensors used for CO<sub>2</sub> gas sensing in biotechnological applications are based on electrochemical measurements that can be prepared with different materials. Optical based CO<sub>2</sub> sensors, with low limits of detection, find applications in a variety of industrial processes, environmental monitoring, pollution control, biotechnology and within the food industry [12]. They are based on the Lewis acid character of CO<sub>2</sub> that, through reaction with the Lewis donor water, causes a change in pH that can be monitored using absorbance or fluorescence-based pH indicators. Typically, the acid-base indicators are immobilized in so-called solid sensor membranes [13], made from gas-permeable polymers such as ethyl cellulose [14], sol-gels [15], silicones [16], composite materials [17] or directly attached to the tip at the end of, or in the core, of an optical fiber [18]. In addition to indicator, the membrane often contains quaternary ammonium hydroxide [19] and/or room-temperature ionic liquids [20;21] for ion pairing with the basic form of the pH indicator, and to provide the water that is needed to form the hydrated ionic pair to uptake the CO<sub>2</sub> from the atmosphere, by forming a lipophilic hydrogencarbonate buffer.

Sensing CO<sub>2</sub> schemes based on luminescence typically result in higher sensitivity than those based on absorption or reflection, although the small number of luminescent acid-base indicators require other strategies such as FRET (fluorescence resonance energy transfer) from an inert fluorescent dye to a colorimetric acid-base indicator, converting the color change in intensity or lifetime information

[13;15;22]. An interesting example in food industry applications is the use of a fluorescence sensor, hydroxypyrene trisulphonate, for the measurement of CO<sub>2</sub> in modified atmosphere packaging by a dual luminophore referencing sensing scheme [23;24].

However, portable instruments for CO<sub>2</sub> detection tend to employ luminescence lifetime-measurements because of their advantages (photobleaching or leaching of the dye, intrinsic sample fluorescence, changes in the light source intensity do not affect the signal) over intensity-based schemes. Phase modulation techniques can be used to implement lifetime-based measurement in portable instrumentation based on phase measurement electronics in conjunction with LEDs and photodiodes [25-28].

Another strategy for CO<sub>2</sub> sensing is based on a colour change conversion to luminescence. It exploits a secondary inner-filter effect of a long lifetime luminophore dye, platinum octaethylporphyrin, immobilized on PVCD membranes, by a pH indicator,  $\alpha$ -naphtholphthalein. It is implemented in a portable instrumentation with both optoelectronic components coated with sensing chemistry (LED with the luminophore and photodetector with the pH-active dye) [29], and later integrated into a multi-analyte platform for oxygen and CO<sub>2</sub> [30].

Contributing factors from both the chemical layer fabrication process and the optical detection system have significant impact on the sensitivity and reproducibility of the sensing device. By employing the most suitable optical detection method sensitivity issues can be addressed. Methods such as charge coupled devices [31], light wave multimeters [19], flat bed scanners [32-34] and photodiodes [35-37] have been explored previously. While functional, not all are suitable for the applications outlined earlier in terms of practicality, portability and scalability. Previous reports by Lau [38], Shepherd [39] and O'Toole *et al.* [40] have reported the advantages of implementing a paired emitter-detector diode (PEDD) arrangement as a colorimetric chemical detection system. A PEDD system consists of two LEDs wherein one is used as the light source (emitter) and the other is used in reverse bias as the light detector.

In this paper we explore the PEDD method along with the  $\alpha$ -naphtholphthalein-platinum octaethylporphyrin chemistry to develop a portable, low-power optical system for CO<sub>2</sub> detection. In this technique the photocurrent generated by the emitter LED and later modified by the sample, discharges the detector LED at a rate which is related to the intensity of light that reaches the detector, which can be tracked by a simple microprocessor circuit. Therefore, instead of measuring the photocurrent directly, a simple timer circuit is used to measure the time taken for the photocurrent generated by the emitter LED to discharge the detector LED to give a digital output directly without using an A/D converter or operation amplifier [41-43].

## 2. EXPERIMENTAL

### Reagents, materials and apparatus

The reagents used were platinum octaethylporphyrin complex (PtOEP, Porphyrin Products Inc., Logan, UT, USA), tributyl phosphate (TBP),  $\alpha$ -naphtholphthalein, and tetraoctyl ammonium hydroxide (TOAOH; 0.335 M in methanol) all from Sigma-Aldrich Química S.A. (Madrid, Spain). The solvents used, tetrahydrofuran (THF), toluene and ethanol, were supplied by Sigma as well. Poly (vinylidene chloride-co-vinyl chloride) (PVCD, particle size 240-320  $\mu$ m) and ethylcellulose (EC, ethoxyl content 49%), were obtained from Sigma. All cocktails were prepared by weighing the chemicals with a DV215CD balance (Ohaus Co., Pine Brook, NJ, USA) which had a precision of  $\pm 0.01$  mg. The gases CO<sub>2</sub> and N<sub>2</sub> were of a high purity (>99%) and were supplied in gas cylinders by Air Liquid S.A. (Madrid, Spain).

The interchangeable membrane platform was fabricated using a laser ablation system-excimer/CO<sub>2</sub> laser, Optec Laser Micromachining Systems, Belgium and a laminator system Titan-110, GBC, USA. 150  $\mu$ m PMMA sheets were purchased from Goodfellow, UK; 50  $\mu$ m double-sided pressure sensitive adhesive film (AR8890) was obtained from Adhesives Research, Ireland and Mylar-type polyester from Goodfellow, UK.

### Portable electronic instrument and signal processing

The realisation of a PEDD instrument for this study consisted of two key elements: 1) Mechanical testing rig; 2) Electronics and control.

Firstly, a test rig was constructed to ensure the accurate alignment of the two LED pair channels, the secure placement of the chemical sensing membrane and to investigate the effect of the distance between the emitter and detector LEDs. Figure 1 illustrates the experimental setup. The membrane housing (constructed using a Dimension SST 768 rapid prototyper) contained two sensing chambers wherein each

was fitted with one LED emitter/detector pair. Furthermore, the chambers were designed with hollow through-hole sections to allow for a flow of gas to react with the sensing membrane. The LEDs were polished and flattened down, and placed within threaded housings, so that the rotation of the housing inside the tapped holder varied the distance between the emitter and the detector. The distance was adjusted by inserting different sized washers, each of a pre-set designed thickness. Finally, the membrane holder allows the sensing surface to be directly aligned with both the emitter and detector LEDs. This design was chosen in order to enable the distance between the emitter and detector to be accurately adjusted.

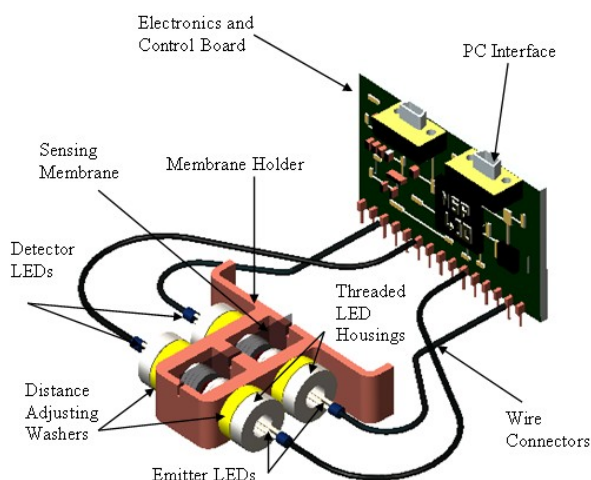


**Figure 1.** Instrumentation setup for the PEDD system. The sensing membrane, equipped with the chemical sensing layer, is held in place by the Membrane Holder and aligned on one axis with the detector/emitter LEDs for absorbance measurements. The LED distances are adjusted via screw threads and/or washers. The control board connects via shielded wiring to the LEDs and reports the measurement values to a PC via the PC interface.

An appropriate electronic design was put in place to realise the operation of a PEDD analysis system. Figure 2 shows that the microcontroller has full control over the operational timing of both detector and emitter LEDs (via IO ports).

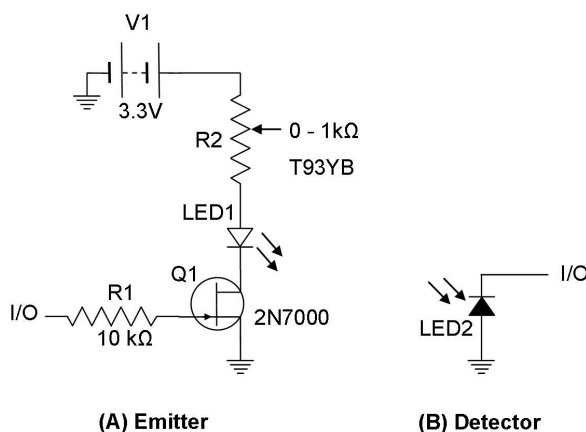


**Figure 2.** Electronic design for the LED emitter and detector system connected to input output (I/O) ports on the MSP430F449 microcontroller. (A) Emitter electronic and control design showing the LED light source powered by a 3.3V regulator, protected by an adjustable resistor (VISHAY T93YB 0-1kΩ Trimmer) and controlled by a NFET transistor (STMICROELECTRONICS NFET 2N7000) via a

microcontroller pin. (B) Detector electronic design showing how the cathode of the LED is charged and analysed by an IO pin on the microcontroller.

The measurement procedure was programmed as follows:

1. Set the software counter variable to 0;
2. Set the detector IO pin to output mode;
3. Charge the detector LED's internal capacitance (cathode), by setting the IO output register high (i.e. 3.3V);
4. Switch the IO register to input mode once the LEDs capacitance is fully charged;
5. Set the emitter IO high to turn on the emitter LED;
6. Check over a fixed number of processor counts (in this case 65535) and increment the software counter if the IO pin's state is above the logic threshold;
7. Output the counter value to the PC;
8. Set the emitter IO low to turn off the emitter LED;
9. Repeat the process i.e. go to step 1.

The number of counts above the threshold is proportional to the time required to discharge the detector LED to the pre-set threshold. This process was repeated and the microcontroller was programmed in a never ending loop to achieve this. Finally, the output sampling rate was set at 1 data point per second. Subsequently, the chemical sensing layer was initially exposed to two extremes i.e. 100% N<sub>2</sub> and 100% CO<sub>2</sub> where the dynamic range of the detector was maximized by adjusting the variable resistor on the emitter LED (see Figure 2), which in turn maximized the resolution.

To determine the optimum distance between emitter LED and detector LED when using the prototype instrument, a study of its response at different distances to 100% N<sub>2</sub> ( $t_0$ ) and 100% CO<sub>2</sub> ( $t_{100}$ ) was carried out. The distances studied were measured from the tip of one LED to the tip of the other, as is explained above.

The  $t_0-t_{100}$  signal increases with distance up to 0.7 mm because of the quantity of light that reaches the detector LED decreases taking into account their viewing angle and thus increasing the discharge time. The optimum operation distance was selected to be 0.7 mm (Figure 3) because the corresponding signal was the largest that was independent of the LED-LED distance.

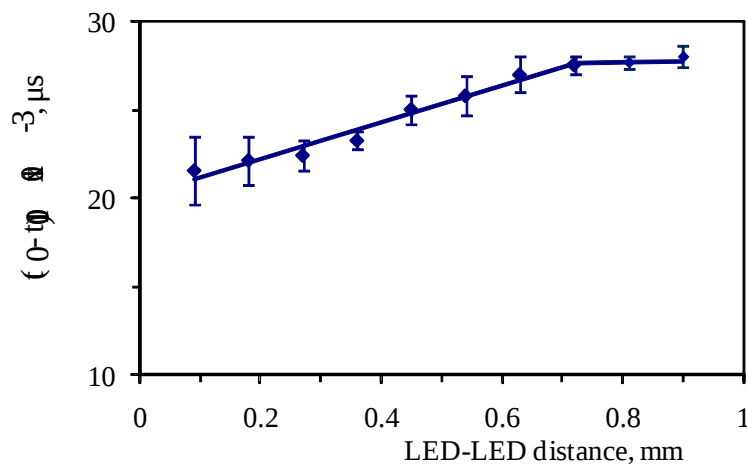


**Figure 3.** Influence of LED-LED distance in the instrument on  $t_0-t_{100}$  value.

### Sensing interchangeable membranes preparation

In order to give an extra degree of freedom to the device and therefore provide easy handling of the membranes during preparation and subsequent device integration, it was decided to fabricate an interchangeable membrane support that contains both sensing membranes. The platform was easily fabricated in poly(methyl methacrylate), pressure-sensitive adhesive and Mylar in five layers designed in AutoCAD (2002), cut using CO<sub>2</sub> laser and laminated, see Figure 1.

Configuration 1: Sensing membranes with luminophore for CO<sub>2</sub> were prepared from cocktails A and B. Cocktail A contains 100 mg of PVCD dissolved in 1 mL of freshly distilled THF, using an ultrasonic bath, and 0.5 mg PtOEP. Cocktail B has 64 µL TBP, 320 µL of a solution containing 2.2 mg of α-naphtholphthalein in 2 mL of toluene/EtOH (80:20 v/v), 1 mL of toluene containing 60 mg of previously dissolved EC, and 200 µL of 0.335 M TOAOH. The sensor preparation consists of the casting on one side of the support with 10 µL of cocktail A. After that, the support was left to dry in darkness in a dryer that had a saturated THF atmosphere for 1 h at room temperature. The prepared PtOEP membranes need to be cured in darkness for 9 days before continuing the preparation. Then, 10 µL of cocktail B was cast on the opposite side of the support with the aid of a micropipette, followed by drying in darkness under a vacuum in a dryer for 12 h at room temperature. The supports were kept in a desiccator in darkness at 94% RH atmosphere (20±0.5°C). The separation between the two membranes is defined by the thickness of the Mylar, 250 µm.

Configuration 2: Sensing membranes without luminophore were prepared by casting 10 µL of cocktail B onto the support, and dried and stored as indicated above.

### Measurement conditions

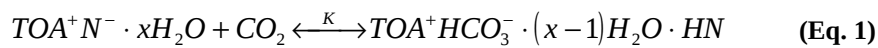
The standard mixtures for instrument calibration and characterization were prepared using N<sub>2</sub> as the inert gas by controlling the flow rates of the different high purity gases CO<sub>2</sub> and N<sub>2</sub>, entering a mixing chamber using a computer-controlled mass flow controller (Air Liquid España S.A., Madrid, Spain) operating at a total pressure of 760 Torr and a flow rate of 500 cm<sup>3</sup>·min<sup>-1</sup>. For the preparation of gas mixtures lower than 2% in CO<sub>2</sub>, a standard mixture of 5% CO<sub>2</sub> in N<sub>2</sub> was used, with the lowest CO<sub>2</sub> concentration tested being 0.1%. For the portable instrument characterization, the measurements were performed after equilibration of the instrument atmosphere for 2 min with the gas mixtures obtained with the gas blender.

All measurements were replicated eight times to check for experimental error. A homemade thermostatic chamber, with a lateral hole for the connexion to a computer and gas tubing entrance, made it possible to maintain a controlled temperature between -50 °C and +50 °C with an accuracy of ±0.5 °C for thermal characterization of the sensor.

## 3. RESULTS AND DISCUSSION

### Optical response of Sensing Membranes

The optical response of the sensor upon exposure to CO<sub>2</sub> is based on its reaction with the deprotonated form of α-naphtholphthalein (N<sup>-</sup>) which is as an ion-pair with tetraoctylammonium (TOA<sup>+</sup>) according to:



where TOA<sup>+</sup>N<sup>-</sup>·xH<sub>2</sub>O is the hydrated ion pair and K the equilibrium constant.

Two different systems were tested in order to find the best conditions to measure CO<sub>2</sub> via the PEDD technique. In the first case, a secondary inner-filter effect accounts for CO<sub>2</sub> sensitivity, as demonstrated previously [29]. It involves the absorption of the phosphorescence emitted from the CO<sub>2</sub>-insensitive luminophore (PtOEP) (λ<sub>exc</sub> 537 nm, λ<sub>em</sub> 650 nm) by the basic form of α-naphtholphthalein (λ<sub>max</sub> 655 nm). This means that a green LED (527 nm) should be used to excite PtOEP that emits around 650 nm so that the emitted radiation is effectively absorbed by the basic form of the indicator (Figure 4). Consequently, a red LED (657 nm) must be used as detector. The increase in CO<sub>2</sub> concentration displaces the equilibrium to the acid form of the indicator (λ<sub>max</sub> 310 nm) increasing the amount of light, from PtOEP phosphorescence, that strikes the detector LED. This reduces the measured discharge time t, which is in turn related to the concentration of the target species.

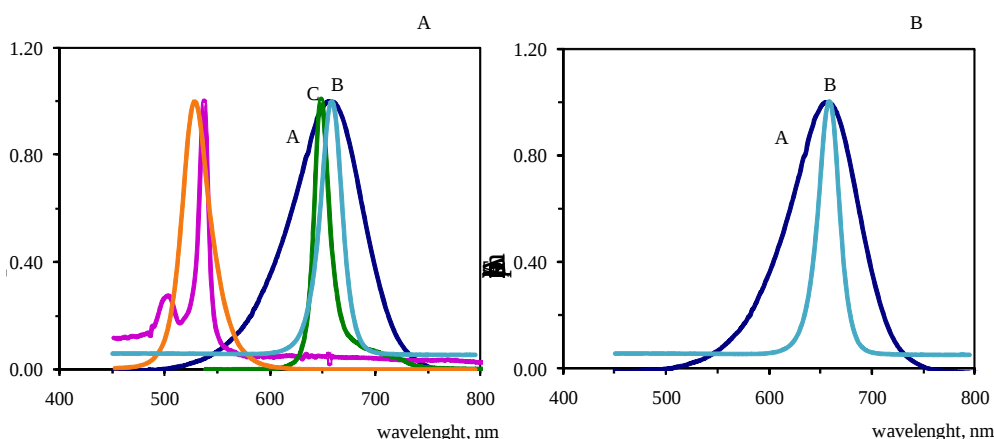


**Figure 4.** Spectral properties of the dyes used in the CO<sub>2</sub> sensing membranes and the excitation source (normalized spectra). Fig.1A. Excitation (E) and phosphorescence emission spectra (C) of PtOEP membrane; (A) absorption spectrum of basic form of  $\alpha$ -naphtholphthalein;(D) emission spectra green LED and (B) emission spectra of red LED. The figure shows the overlapping of donor and acceptor spectra. Fig. 4B. (A) absorption spectrum of basic form of  $\alpha$ -naphtholphthalein and (B) emission spectra of red LED.

The opposite side configuration for both luminophore and pH indicator membranes is used to prevent the observed degradation of the PtOEP complex in the presence of the phase transfer agent, TOAOH. However, degradation is observed even if the platinum complex is included in microparticles [29]. Additionally, the immobilization of PtOEP in oxygen-insensitive PVCD membrane prevents their quenching by oxygen at atmospheric level.

In the second system tested, the membrane containing the luminophore PtOEP is eliminated, simplifying the sensing membrane that now only contains the acid-base indicator, reducing cost and completely avoiding the interference of O<sub>2</sub> upon the phosphorescence of the PtOEP complex. This second system is formed by mounting two identical red LEDs (657 nm) facing each other, with the holder containing the indicator membrane placed between the two LEDs

#### Instrument response to carbon dioxide

Both sensing membrane systems respond to CO<sub>2</sub> through variations of the ratio of protonated to deprotonated forms of the  $\alpha$ -naphtholphthalein indicator which generate corresponding changes in the discharge time of the reverse biased detector LED, which are related to the CO<sub>2</sub> concentration. Plotting the discharge time versus CO<sub>2</sub> percentage gives a decay function that can be fitted to the exponential function  $y = y_0 + Ae^{-(x/t)}$  (configuration 1: R<sup>2</sup>=0.9983, configuration 2: R<sup>2</sup>=0.9845).

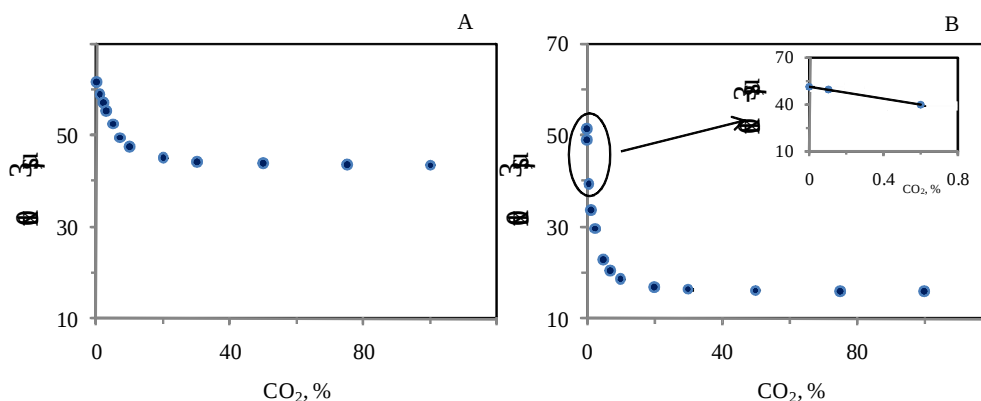


**Figure 5.** Response of the instrumental prototype to CO<sub>2</sub>. Discharge time vs. CO<sub>2</sub> percentage. A: configuration 1 and B: configuration 2. Inset: Experimental function used to calculate the LOD.

According to Mills *et al.* [44] the ratio of concentrations of protonated to deprotonated forms of indicator is proportional to CO<sub>2</sub> concentration:

$$\frac{[TOA^+HCO_3^- \cdot (x-1)H_2O \cdot HN]}{[TOA^+N^- \cdot xH_2O][CO_2]} = K[CO_2] = \frac{A_0 - A}{A - A_{100}} \quad (\text{Eq. 2})$$

where A<sub>0</sub> and A<sub>100</sub> are the absorbance at 0 (deprotonated form) and 100 % CO<sub>2</sub> (protonated form), respectively, and A is the absorbance at any intermediate concentration.

The absorbance was calculated from eq. 3 using the amount of light I reaching the detector and the amount I<sup>0</sup> in the absence of indicator membrane [41]. The value t<sup>0</sup> corresponds to the discharge time obtained in the absence of the indicator membrane and t to the discharge time of the membrane at any CO<sub>2</sub> concentration.

$$A = \log \frac{I^0}{I} = -\log \frac{t^0}{t} \quad (\text{Eq.3})$$

From eq. 2 a linear relationship can be obtained with slope equal K and zero intercept. The deviations observed at higher CO<sub>2</sub> percentages can be attributed to non fulfillment of Beer's law due to use of a

polychromatic light source in this instrument. (Configuration 1:  $\frac{A_0 - A}{A - A_{100}} = 0.1703[CO_2] - 0.0286$ ;

R<sup>2</sup>= 0.9901; Configuration 2:  $\frac{A_0 - A}{A - A_{100}} = 0.4467[CO_2] - 0.021$ ; R<sup>2</sup> = 0.9857).

The slopes found show that a considerable difference in sensitivity exists between both configurations (configuration 2 is 2.6 times more sensitive than configuration 1).

### Comparison between the two configurations studied

It is possible to use the above eq. 2 for calibration purposes although the linear response is limited up to ca. 5 %. Moreover to achieve a full calibration range, that could be included in the microcontroller of the instrument, an empirical equation was used based on a relative analytical parameter (named as R) based on the discharge time ( $(t_{100} - t_0)/(t - t_0)$ ) vs. the inverse of CO<sub>2</sub> concentration. In this case t<sub>0</sub> and t<sub>100</sub> are the values of discharge time at 0 and 100 % CO<sub>2</sub>, respectively and t at any other concentration.

The limit of detection (LOD) of the instrumental procedure was obtained from exponential raw experimental data using the first three points at low CO<sub>2</sub> concentration because they can be adjusted to a straight line (Figure 5 inset) [45]. Using the critical level (s<sub>0</sub>) in the signal domain (configuration 1: 50.91 μs; configuration 2: 108.73 μs) and the obtained adjustments (configuration 1: t = -2290.1[CO<sub>2</sub>] + 61535; R<sup>2</sup>=0.989; configuration 2: t = -19525[CO<sub>2</sub>] + 51155; R<sup>2</sup>=0.999) the LODs were calculated as usual by LOD = t<sub>0</sub> + 3 s<sub>0</sub>, where t<sub>0</sub> is the average blank signal (previously defined) and s<sub>0</sub> is the critical level or standard deviation of the blank, which was determined from eight replicate measurements. The LODs found using this approach were 0.0082 % for configuration 1 and 0.0066 % for configuration 2 (notice that this value is less than normal atmospheric CO<sub>2</sub> concentration, which is ca. 0.04%).

The limit of quantification (LOQ) was obtained from the calibration function [46]. In this case the critical level s<sub>0</sub> is the standard deviation of t<sub>0</sub>, the discharge time at the LOQ as given by equation 4, and the analytical parameter at the LOQ (R<sub>LOQ</sub>) as given by equation 5. Therefore, from the obtained R<sub>LOQ</sub> and the calibration function the LOQ can be estimated as 5.9% and 2.6% CO<sub>2</sub> for configurations 1 and 2, respectively.

$$t_{LOQ} = t_0 - 10s_0 \quad (\text{Eq. 4})$$

$$R_{LOQ} = \frac{t_{100} - t_0}{10s_0} \quad (\text{Eq. 5})$$

The comparison between both configurations studied, in terms of signal range (t<sub>0</sub>-t<sub>100</sub>), and slope of calibration function, LOD and LOQ (Table 1) shows configuration 2 gives better performance. The difference between the behaviour of the two configurations can be explained by considering that the use of the luminiscent membrane in configuration 1 reduces the amount of light reaching the sensing

membrane and hence the detector LED compared to configuration 2. Hence configuration 2 was selected for subsequent experiments.

**Table 1.** Comparison of signal range, slope, LOD and LOQ of the two sensing configurations studied.

	$t_0-t_{100}$ ( $\mu$ s)	Slope	LOD (%)	LOQ (%)
Configuration 1	18,175	5.962	0.0082	5.86
Configuration 2	35,358	1.379	0.0066	2.67

### Analytical characterization

The dynamic response of the sensing membranes when exposed to alternating atmospheres of pure CO<sub>2</sub> and pure nitrogen was carried out as shown in Figure 6. The response time was calculated from between 10% and 90% of the maximum signal, returning a value of  $11.0 \pm 0.9$  s and, the recovery time from 90% to 10% which was found to be  $55.3 \pm 4.8$  s.

In addition, the response and recovery behaviour of the CO<sub>2</sub> sensing membrane was studied at different intermediate CO<sub>2</sub> concentrations (0, 1, 3, 7, 20, 100% CO<sub>2</sub>). In all cases, the signal changes were fully reversible and hysteresis was not observed during the measurements.

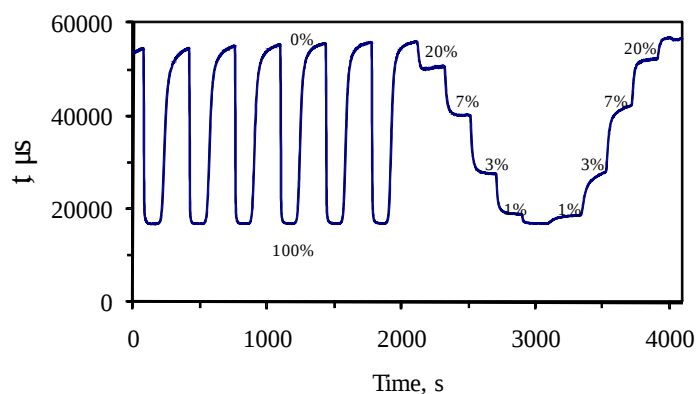


**Figure 6.** Dynamic response of the portable instrument to changes in CO<sub>2</sub> concentration from 0% to 100%. Response characteristics at 1, 3, 7, 20 and 100% CO<sub>2</sub>.

The response and recovery times are lower than those obtained for other systems developed by us [29;30;47], especially the recovery time, which was half of that obtained before. The response and recovery times obtained here are comparable and even lower than other sensing schemes widely used for CO<sub>2</sub> sensing [48-50].

The precision of proposed prototype was measured by studying the intra-day reproducibility. Five measurements at 100% N<sub>2</sub> and 100% CO<sub>2</sub> were performed using the same membrane at 45 minutes intervals with 8 replicates each. A good reproducibility with a relative standard deviation of 1.15% was obtained for  $t_0-t_{100}$ .

Stability is a very important characteristic to take into account in a sensor, and even more so if this device is going to be used for industrial applications. Stability was studied by means of an inter-day reproducibility measuring  $t_0$  and  $t_{100}$  (with the same membrane as in the intra-day study) repeated for 5 days in a row ( $n=8$  per day). The inter-day relative standard deviation was 1.77%, in good agreement with our previous study of the stability of  $\alpha$ -naphtholphthalein membrane, in which a one year long-term stability of the indicator membrane was demonstrated when stored under 94% RH conditions [47].

Temperature has a considerable influence on the sensitivity of CO<sub>2</sub> sensors based on CO<sub>2</sub> acid-base character [44;51]. Therefore, we studied the thermal dependence of the sensing membranes by acquiring the calibration function at temperatures between 5 °C and 30 °C. From this study, we observed a decrease

in sensitivity with increasing temperature (Figure 7), which can be attributed to the inverse dependence of the CO<sub>2</sub> solubility in the indicator layer on the temperature [52].

By using eq. 2 and 3 the value of K was calculated for each temperature and the resulting ln K vs. T<sup>-1</sup> (Kelvin degrees) plot up to 5% CO<sub>2</sub> was linear (R<sup>2</sup> = 0.995, Inset figure 6) yielding a ΔH value of -142 KJ/mol and a ΔS of -208 J/mol·K. Here ΔG<0, that means that the reactions are spontaneous, due to the large negative ΔH value as was observed previously with similar sensors [44;53].

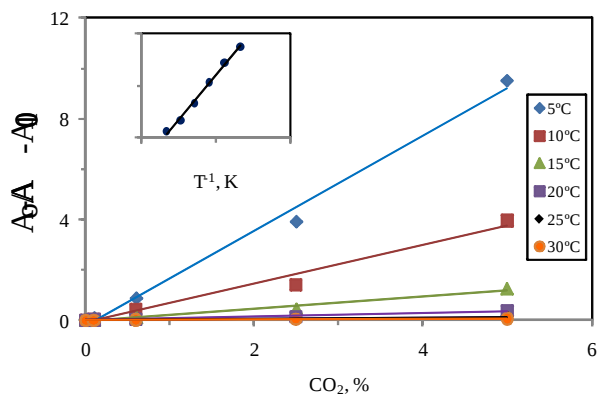


**Figure 7.** Thermal dependence of the sensing membranes. Main section: Plots of  $\frac{A_0 - A}{A - A_{100}}$  vs. CO<sub>2</sub> percentage at each temperature studied (5-30°C). Inset: plot of lnK vs. T (K) over the temperature range studied.

## CONCLUSIONS

The instrumental design studied could form the basis of a versatile handheld instrument for industrial applications, capable of measuring very low CO<sub>2</sub> concentrations, to below atmospheric value, and up to 1%, due to the good precision achieved. In addition, a much broader CO<sub>2</sub> range (from 2.6 to 100%) can be measured by means a relative signal.

Two different configurations have been tested, with configuration 2 being the most sensitive. This configuration comprises two red LEDs, one LED working as emitter and the other one as detector. The interchangeable sensor layer only contains α-naphtholphthalein (the PtOEP membrane is eliminated) which brings advantages like simplification of the sensing membrane, reduced cost and avoidance of the O<sub>2</sub> interference on the analytical signal arising from phosphorescence of the PtOEP complex.

Some advantages of the PEDD arrangement include the simplicity of the resulting sensor and electronics, low cost, high resolution, and excellent sensitivity.

The device has been characterised in terms of sensitivity, dynamic response, reproducibility, stability and temperature influence.

The response and recovery times found were very fast in comparison with other devices based on the acidic nature of CO<sub>2</sub>. The signals were fully reversible, and hysteresis was not observed during measurements. Moreover, good reproducibility and stability have been found. The temperature influence was studied and modelled; a normal behaviour was found and demonstrated for this prototype.

The characterisation suggests that overall this is a very promising sensor for monitoring CO<sub>2</sub>.

## REFERENCES

- [1] M. Mazzotti, J. C. Abanades, R. Allam, K. S. Lackner, F. Meunier, E. Rubin, J. C. Sanchez, K. Yogo, and R. Zevenhoven, "Mineral carbonation and industrial uses of carbon dioxide," in *IPCC Special Report on Carbon Dioxide Capture and Storage*. e. a. E. B. Metz, Ed. NY: Cambridge University Press, 2005, pp. 319-338.
- [2] M. Sivertsvik, W. K. Jeksrud, and J. T. Rosnes, "A review of modified atmosphere packaging of fish and fishery products - significance of microbial growth, activities, and safety," *Int. J. Food Sci. Technol.*, vol. 37, no. 2, pp. 107-127, 2002.
- [3] S. Neethirajan, D. S. Jayas, and S. Sadistap, "Carbon dioxide (CO<sub>2</sub>) sensors for the agri-food industry-a review," *Food Bioprocess Technol.*, vol. 2, no. 2, pp. 115-121, 2009.
- [4] S. C. Seideman and P. R. Durland, "The utilization of modified gas atmosphere packaging for fresh meat: a review," *J. Food Qual.*, vol. 6, no. 3, pp. 239-252, 1984.
- [5] P. Suppakul, J. Miltz, K. Sonneveld, and S. W. Bigger, "Active packaging technologies with an emphasis on antimicrobial packaging and its applications," *J. Food Sci.*, vol. 68, no. 2, pp. 408-420, 2003.
- [6] M. Ozdemir and J. D. Floros, "Active food packaging technologies," *Crit. Rev. Food Sci. Nutr.*, vol. 44, no. 3, pp. 185-193, 2004.
- [7] J. P. Kerry, M. N. O'Grady, and S. A. Hogan, "Past, current and potential utilisation of active and intelligent packaging systems for meat and muscle-based products: A review," *Meat Science*, vol. 74, no. 1, pp. 113-130, Sept.2006.
- [8] M. L. Rooney, *Active food packaging*. Glasgow: Blackie Academic & Professional, 1995.
- [9] G. Zhang and X. Wu, "A novel CO<sub>2</sub> gas analyzer based on IR absorption," *Opt. Lasers Eng.*, vol. 42, no. 2, pp. 219-231, Aug.2004.
- [10] J. W. Fergus, "A review of electrolyte and electrode materials for high temperature electrochemical CO<sub>2</sub> and SO<sub>2</sub> gas sensors," *Sens. Actuators B*, vol. 134, no. 2, pp. 1034-1041, 2008.
- [11] H. H. Moebius, "Galvanic solid electrolyte cells for the measurement of CO<sub>2</sub> concentrations," *J. Solid State Electrochem.*, vol. 8, no. 2, pp. 94-109, 2004.
- [12] V. Vojinovic, J. M. S. Cabral, and L. P. Fonseca, "Real-time bioprocess monitoring," *Sens. Actuators B*, vol. 114, no. 2, pp. 1083-1091, 2006.
- [13] A. Mills and K. Eaton, "Optical sensors for carbon dioxide: an overview of sensing strategies past and present," *Quim. Anal.*, vol. 19, no. Supl. 1, pp. 75-86, 2000.
- [14] N. Nakamura and Y. Amao, "Optical sensor for carbon dioxide combining colorimetric change of a pH indicator and a reference luminescent dye," *Anal. Bioanal. Chem.*, vol. 376, no. 5, pp. 642-646, 2003.
- [15] C. v. Bültzingslöwen, A. K. McEvoy, C. McDonagh, and B. D. MacCraith, "Lifetime-based optical sensor for high-level pCO<sub>2</sub> detection employing fluorescence resonance energy transfer," *Anal. Chim. Acta*, vol. 480, pp. 275-283, 2003.
- [16] X. Ge, Y. Kostov, and G. Rao, "High-stability non-invasive autoclavable naked optical CO<sub>2</sub> sensor," *Biosensors Bioelectron.*, vol. 18, no. 7, pp. 857-865, July2003.

- [17] S. M. Borisov, C. Krause, S. Arain, and O. S. Wolfbeis, "Composite material for simultaneous and contactless luminescent sensing and imaging of oxygen and carbon dioxide," *Adv. Mater.*, vol. 18, no. 12, pp. 1511-1516, 2006.
- [18] F. Baldini, A. Giannetti, A. A. Mencaglia, and C. Trono, "Fiber optic sensors for biomedical applications," *Curr. Anal. Chem.*, vol. 4, no. 4, pp. 378-390, 2008.
- [19] B. H. Weigl and O. S. Wolfbeis, "Sensitivity studies on optical carbon dioxide sensors based on ion pairing," *Sens. Actuators B*, vol. 28, no. 2, pp. 151-156, Aug.1995.
- [20] S. M. Borisov, M. C. Waldhier, I. Klimant, and O. S. Wolfbeis, "Optical Carbon Dioxide Sensors Based on Silicone-Encapsulated Room-Temperature Ionic Liquids," *Chem. Mater.*, vol. 19, no. 25, pp. 6187-6194, 2007.
- [21] O. Oter, K. Ertekin, and S. Derinkuyu, "Ratiometric sensing of CO<sub>2</sub> in ionic liquid modified ethyl cellulose matrix," *Talanta*, vol. 76, no. 3, pp. 557-563, 2008.
- [22] G. Neurauder, I. Klimant, and O. S. Wolfbeis, "Microsecond lifetime-based optical carbon dioxide sensor using luminescence resonance energy transfer," *Anal. Chim. Acta*, vol. 382, no. 1-2, pp. 67-75, Feb.1999.
- [23] C. v. Bültzingslöwen, A. K. McEvoy, C. McDonagh, B. D. MacCraith, I. Klimant, K. Christian, and O. S. Wolfbeis, "Sol-gel based optical carbon dioxide sensor employing dual luminophore referencing for application in food packaging technology," *Analyst*, vol. 127, no. 11, pp. 1478-1483, Oct.2002.
- [24] A. K. McEvoy, B. D. MacCraith, C. McDonagh, and C. von Buelzingsloewen, "Optical CO<sub>2</sub> and combined O<sub>2</sub>/CO<sub>2</sub> sensors," WO/2004/077035, 2010.
- [25] D. Kieslinger, K. Trznadel, K. Oechs, S. Draxler, and M. E. Lippitsch, "Lifetime-based portable instrument for blood gas analysis," *Proc. SPIE-Int. Soc. Opt. Eng.*, vol. 2976, no. Biomedical Sensing, Imaging, and Tracking Technologies II, pp. 71-77, 1997.
- [26] M. E. Lippitsch, D. Kieslinger, and S. Draxler, "Luminescence lifetime-based sensing: New materials, new devices," *Sens. Actuators B*, vol. 38, no. 1-3, pp. 96-102, 1997.
- [27] C. Malins, M. Niggemann, and B. D. MacCraith, "Multi-analyte optical chemical sensor employing a plastic substrate," *Meas. Sci. Technol.*, vol. 11, no. 8, pp. 1105-1110, 2000.
- [28] O. McGaughey, R. Nooney, A. K. McEvoy, C. McDonagh, and B. D. MacCraith, "Development of a multi-analyte integrated optical sensor platform for indoor air-quality monitoring," *Proc. SPIE-Int. Soc. Opt. Eng.*, vol. 5993, no. Advanced Environmental, Chemical, and Biological Sensing Technologies III, pp. 59930R-1-59930R/12, 2005.
- [29] I. M. Perez de Vargas-Sansalvador, M. A. Carvajal, O. M. Roldan-Munoz, J. Banqueri, M. D. Fernandez-Ramos, and L. F. Capitan-Vallvey, "Phosphorescent sensing of carbon dioxide based on secondary inner-filter quenching," *Anal. Chim. Acta*, vol. 655, no. 1-2, pp. 66-74, 2009.
- [30] I. M. Perez de Vargas-Sansalvador, A. Martinez-Olmos, A. J. Palma, M. D. Fernandez-Ramos, and L. F. Capitan-Vallvey, "Compact optical instrument for simultaneous determination of oxygen and carbon dioxide," *Mikrochim. Acta*, vol. DOI 10.1007/s00604-010-0520-0 2011.
- [31] J. C. Carter, R. M. Alvis, S. B. Brown, K. C. Langry, T. S. Wilson, M. T. McBride, M. L. Myrick, W. R. Cox, M. E. Grove, and B. W. Colston, "Fabricating optical fiber imaging sensors using inkjet printing technology: A pH sensor proof-of-concept," *Biosensors Bioelectron.*, vol. 21, no. 7, pp. 1359-1364, 2006.
- [32] M. C. Janzen, J. B. Ponder, D. P. Bailey, C. K. Ingison, and K. S. Suslick, "Colorimetric Sensor Arrays for Volatile Organic Compounds," *Anal. Chem.*, vol. 78, no. 11, pp. 3591-3600, 2006.

- [33] N. A. Rakow and K. S. Suslick, "A colorimetric sensor array for odour visualization," *Nature*, vol. 406, no. 6797, pp. 710-713, 2000.
- [34] N. A. Rakow, A. Sen, M. C. Janzen, J. B. Ponder, and K. S. Suslick, "Molecular recognition and discrimination of amines with a colorimetric array," *Angew. Chem. Int. Ed.*, vol. 44, no. 29, pp. 4528-4532, 2005.
- [35] K. Crowley, A. Pacquit, J. Hayes, L. King Tong, and D. Diamond, "A gas-phase colorimetric sensor for the detection of amine spoilage products in packaged fish," *IEEE Sens.*, n° 2, 754-757, 2005.
- [36] A. Pacquit, J. Frisby, D. Diamond, K. T. Lau, A. Farrell, B. Quilty, and D. Diamond, "Development of a smart packaging for the monitoring of fish spoilage," *Food Chem.*, vol. 102, no. 2, pp. 466-470, 2007.
- [37] A. Pacquit, K. T. Lau, H. McLaughlin, J. Frisby, B. Quilty, and D. Diamond, "Development of a volatile amine sensor for the monitoring of fish spoilage," *Talanta*, vol. 69, no. 2, pp. 515-520, 2006.
- [38] K.-T. Lau, S. Baldwin, M. O'Toole, R. Shepherd, W. J. Yerazunis, S. Izuo, S. Ueyama, and D. Diamond, "A low-cost optical sensing device based on paired emitter-detector light emitting diodes," *Anal. Chim. Acta*, vol. 557, no. 1-2 2006.
- [39] R. Shepherd, S. Beirne, K. T. Lau, B. Corcoran, and D. Diamond, "Monitoring chemical plumes in an environmental sensing chamber with a wireless chemical sensor network," *Sens. Actuators B*, vol. 121, no. 1, pp. 142-149, 2007.
- [40] M. O'Toole, R. Shepherd, G. G. Wallace, and D. Diamond, "Inkjet printed LED based pH chemical sensor for gas sensing," *Anal. Chim. Acta*, vol. 652, no. 1-2, pp. 308-314, 2009.
- [41] K. T. Lau, S. Baldwin, R. L. Shepherd, P. H. Dietz, W. Yerzunis, and D. Diamond, "Novel fused-LEDs devices as optical sensors for colorimetric analysis," *Talanta*, vol. 63, no. 1, pp. 167-173, 2004.
- [42] M. O'Toole and D. Diamond, "Absorbance based light emitting diode optical sensors and sensing devices," *Sensors*, vol. 8, no. 4, p. No, 2008.
- [43] R. L. Shepherd, W. S. Yerazunis, K. T. Lau, and D. Diamond, "Low-cost surface-mount LED gas sensor," *IEEE Sens. J.*, vol. 6, no. 4, pp. 861-866, 2006.
- [44] A. Mills, A. Lepre, and L. Wild, "Breath-by-breath measurement of carbon dioxide using a plastic film optical sensor," *Sens. Actuators B*, vol. 39, no. 1-3, pp. 419-425, Mar.1997.
- [45] ISO, "Capability of detection. Methodology in the linear and non-linear cases," *Internacional standard. ISO11843-5*, 2008.
- [46] IUPAC, "Nomenclature in evaluation of analytical methods including detection and quantification capabilities (IUPAC Recommendations 1995)," *Pure Appl. Chem.*, vol. 67, no. 10, pp. 1699-1723, 1995.
- [47] M. A. Carvajal, I. M. Perez de Vargas Sansalvador, A. J. Palma, M. D. Fernandez-Ramos, and L. F. Capitan-Vallvey, "Hand-held optical instrument for CO<sub>2</sub> in gas phase based on sensing film coating optoelectronic elements," *Sens. Actuators B*, vol. B144, no. 1, pp. 232-238, 2010.
- [48] K. Ertekin, I. Klimant, G. Neurauter, and O. S. Wolfbeis, "Characterization of a reservoir-type capillary optical microsensor for pCO<sub>2</sub> measurements," *Talanta*, vol. 59, no. 2, pp. 261-267, 2003.
- [49] C. Malins and B. D. MacCraith, "Dye-doped organically modified silica glass for fluorescence based carbon dioxide gas detection," *Analyst*, vol. 123, no. 11, pp. 2373-2376, Nov.1998.

- [50] D. A. Nivens, M. V. Schiza, and S. M. Angel, "Multilayer sol-gel membranes for optical sensing applications: single layer pH and dual layer CO<sub>2</sub> and NH<sub>3</sub> sensors," *Talanta*, vol. 58, no. 3, pp. 543-550, 2002.
- [51] A. Mills and L. Monaf, "Thin Plastic Film Colorimetric Sensors for Carbon Dioxide: Effect of Plasticizer on Response," *Analyst*, vol. 121, pp. 535-540, 1996.
- [52] M. D. Marazuela, M. C. Moreno-Bondi, and G. Orellana, "Enhanced performance of a fiber-optic luminescence CO<sub>2</sub> sensor using carbonic anhydrase," *Sens. Actuators B*, vol. B29, no. 1-3, pp. 126-131, 1995.
- [53] A. Mills, Q. Chang, and N. McMurray, "Equilibrium Studies on Colorimetric Plastic Film Sensors for Carbon Dioxide," *Anal. Chem.*, vol. 64, pp. 1383-1389, 1992.